# Vesicle association and exocytosis at ribbon and extraribbon sites in retinal bipolar cell presynaptic terminals

**David Zenisek***

Department of Cellular and Molecular Physiology, Department of Ophthalmology and Visual Science, Program in Cellular Neuroscience, Neurodegeneration and Repair, Yale University School of Medicine, 333 Cedar Street, SHM-B147, New Haven, CT 06520

Edited by William Betz, University of Colorado School of Medicine, Denver, CO, and accepted by the Editorial Board, accepted February 6, 2008 (received for review September 24, 2007)

**Synaptic vesicles release neurotransmitter by following a process of vesicle docking and exocytosis. Although these steps are well established, it has been difficult to observe and measure these rates directly in living synapses. Here, by combining the direct imaging of single synaptic vesicles and synaptic ribbons, I measure the properties of vesicle docking and evoked and spontaneous release from ribbon and extraribbon locations in a ribbon-type synaptic terminal, the goldfish retinal bipolar cell. In the absence of a stimulus, captured vesicles near ribbons associate tightly and only rarely undock or undergo spontaneous exocytosis. By contrast, vesicle capture at outlier sites is less stable and spontaneous exocytosis occurs at a higher rate. In response to a stimulus, exocytic events cluster near ribbons, but show no evidence of clustering away from ribbon sites. Together, the results here indicate that, although vesicles can associate and fuse both near and away from synaptic sites, vesicles at synaptic ribbons associate more stably and fusion is more tightly linked to stimuli.**

imaging | neurotransmitter release | retina | synapse | synaptic vesicle

Before exocytosis, synaptic vesicles from a cytoplasmic pool must first dock to release sites in active zones of presynaptic terminals. Although the existence of a cohort of vesicles near the membrane has been well established in many neuronal preparations in static electron microscopic images, it has been difficult to study dynamically in living nerve terminals. There have been very few measurements of vesicle undocking at active zones (1) and it would be of interest to directly measure these rates. At ribbon-type synapses of the auditory, vestibular, and visual systems, vesicles are first thought to be captured or "docked" to a "synaptic ribbon," before undergoing exocytosis. Synaptic ribbons are specifically located opposite postsynaptic receptors (2–5) and tethered to each synaptic ribbon is a dense array of synaptic vesicles (6–8). Given this localization and the fact that these structures are specific to nonspiking tonic synapses that release large amounts of neurotransmitter, it has long been suggested that vesicles tethered to the ribbon are recruited to release neurotransmitter in these synapses (9–11). In addition to ribbon-associated release, synaptic vesicles have been suggested to undergo extraribbon release in the goldfish retinal bipolar cells (11, 12), and extraribbon release was suggested to occur primarily at ribbon-free active zones (11). In this study, I combine imaging of single synaptic vesicles and synaptic ribbons to look directly at vesicle undocking and exocytosis at synaptic ribbons and extraribbon sites in the goldfish bipolar cell terminal. Here, I show that vesicles associate more tightly with ribbon sites than at extrasynaptic sites, that spontaneous release is more common extrasynaptically, and that clusters of fusion events colocalize with ribbon sites, but not extraribbon sites. The results here support a model in which the synaptic ribbon serves to direct exocytosis to discrete locations by stabilizing a pool of vesicles near calcium channels.

## Results

**Vesicles Are Preferentially Immobilized and Fuse Near Synaptic Ribbons.** To study the properties of synaptic vesicles in ribbon synapses, bipolar cell vesicles were loaded with the fluorescent dye FM1–43 (13) and imaged by using total internal reflection fluorescence microscopy (TIRFM). By using a brief application of FM1–43 in the presence of a moderately depolarizing stimuli (25 mM KCl), only a small fraction of the total pool was labeled (12, 14). After allowing enough time for excess dye to be washed away (>25 min) in a low-calcium solution, single synaptic vesicles were readily visible in TIRFM. As previously described, most (>90%) vesicles remained visible for <200 ms because of their relatively high mobility (15). By contrast, a subset of vesicles remained immobile for >500 ms. By averaging all images taken from the cell in our experiments, hot spots where vesicles were preferentially captured become visible in most cells (12). An example of these hot spots is shown in Fig. 1*A*. Because vesicles can be seen to be physically tethered to synaptic ribbons in electron micrographs, it is reasonable to hypothesize that some or all of these hot spots may be synaptic ribbons. To test this idea directly, bipolar cells labeled with FM1–43 were loaded with a peptide previously shown to bind to the synaptic ribbon (16) by patch pipette. After loading with the peptide, cell brightness increased ≈10-fold and vesicles were no longer visible. Instead, immobile spots remained, marking the location of synaptic ribbons. TIRFM imaging of the peptide-labeled cells (Fig. 1*B*) indicated a striking colocalization between vesicle-binding sites and synaptic ribbons (Fig. 1*C*).

In the next set of experiments, bipolar cells were stimulated with a brief application of a solution of 25 mM KCl to evoke exocytosis. When challenged with this stimulus, a subset of synaptic vesicles rapidly became brighter followed by the dye emanating radially from the spot, indicating exocytosis (12). These fusion events had a tendency to cluster at discrete locations (data not shown), as has been described for bipolar cells recorded under different experimental conditions (11, 12). To test whether synaptic vesicles preferentially fused at the base of the synaptic ribbon, bipolar cells were next whole-cell voltage-clamped with a pipette solution containing the fluorescent ribbon-binding peptide to determine the location of the ribbons. Fusing vesicles were much more likely to be found near synaptic ribbon sites. Fig. 2 *A–F* shows an example of two events that occurred near two ribbon sites in response to a single stimulus. Fig. 2 *G–J* shows the location of ribbons fluorescently labeled by using the peptide and exocytic sites from the same cells. From

Author contributions: D.Z. designed research, performed research, contributed new reagents/analytic tools, analyzed data, and wrote the paper.

The author declares no conflict of interest.

This article is a PNAS Direct Submission. W.B. is a guest editor invited by the Editorial Board.

*To whom correspondence should be addressed. E-mail: david.zenisek@yale.edu.

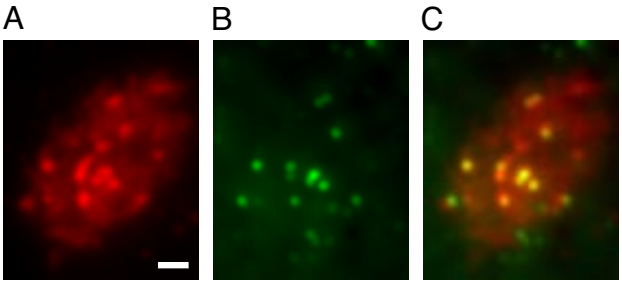


**Fig. 1.** Imaging synaptic vesicles and synaptic ribbons. (*A–C*) Three images from a goldfish retinal bipolar cell loaded with FM1–43 and imaged by using TIRFM. Note the high degree of colocalization of ribbons with vesicle-docking sites, although some ribbon locations (e.g., two green dots at the bottom of *C*) do not correspond to hot spots of vesicle-docking sites, possibly indicating that some ribbons may be nonfunctional. Alternatively, this may mark locations where the footprint of the cell has shifted during the course of the experiment. (Scale bar: 1 $\mu$m.)

this figure, it is apparent that most fusion events cluster to a subset of synaptic ribbons. This is explored more rigorously in Fig. 2 *K–M*. Fig. 2*K* shows a histogram of fusion event distances from the nearest ribbon that includes events evoked by depolarization and spontaneous events, whereas Fig. 2*L* shows a histogram of the expected distribution of distances for a random collection of vesicles and the observed ribbon locations, taking into account the number of fusion events in each cell and the shape of each cell footprint. To look at the relative likelihood of finding a fusion event after taking geometric considerations into account, one can normalize the measured histogram in Fig. 2*K* to the random distribution in Fig. 2*L*. Fig. 2*M* shows these results. From these data it is evident that fusion events do not distribute randomly, but instead vesicles have the highest probability of fusing at locations nearest the ribbon and likelihood decreases with distance from the ribbon. A region extending to ≈700 nm from the center of the ribbons exhibited more events than expected from random. It is noteworthy that this distance is somewhat larger than the ribbon itself. This is most likely due to the slow movement of the ribbon over the time required to do these experiments (10–30 min), which have previously been described (11, 16). In addition to these events near the ribbon, outlier fusion events also occurred away from the ribbon (Fig. 2). In total, 82 of 220 (37%) fusion events were >500 nm from the center of a ribbon and 50 of 220 (23%) fusion events occurred >700 nm away from the nearest ribbon, indicating that exocytosis is not restricted to ribbon sites.

**Vesicle Association and Dissociation at Synaptic Ribbons and Extrasynaptic Sites.** Next, I investigated the properties of vesicle unbinding and spontaneous exocytosis at the ribbon and elsewhere within the terminal. Most vesicles are highly mobile and appear only transiently (<300 ms) when imaged by using TIRFM (12, 15). These vesicles undergo apparently Brownian motion with a diffusion coefficient of 0.01–0.06 $\mu m^2/s$ (15; data not shown). By contrast, a subset of vesicles exhibited little fluctuation in intensity in the absence of a stimulus. To study this population of immobile vesicles, bipolar cells were continually superfused with a low-calcium solution to prevent exocytosis driven by spontaneous calcium action potentials (17, 18) while being imaged by using TIRFM. These experiments were immediately followed by the introduction of the ribbon-binding peptide by whole-cell patch pipette to determine the location of the ribbons. Cells were imaged for 6- to 10-s epochs of continuous image capture and illumination to follow the fate of individual docked vesicles. Vesicles that remained continually visible for >500 ms were selected for further analysis. In 104 s of imaging across 10 cells, 95 vesicles met this criterion. Of these docked vesicles, 41% were found to reside within 500 nm of the center of a ribbon. By comparison, only 10.4% of the footprint surface area is within this distance of a ribbon. Evidently ribbons are preferred locations, but not a requirement, for vesicle capture near the plasma membrane.

Given the distance dependence of fluorescence intensity in TIRF imaging, the movement of the vesicle could contribute to the fluctuation in fluorescence intensity. To evaluate this, vesicle intensities were measured by taking the fluorescence in a circular region encompassing the fluorescent spots and subtracting the fluorescence of a surrounding annulus to estimate and remove the contribution of the local background. To minimize the effects of any lateral movement of vesicles, ribbons, or the synaptic terminal, a region size was chosen that was considerably larger than the vesicles (675 nm). A surrounding annulus of 675–1,500 nm was used to estimate local background. On average, the fluorescence intensity of docked vesicles at ribbons varied with a standard deviation equivalent to 16.0 ± 1.0% (mean ± SE) of their mean intensities and 19.8 ± 1.2% of the mean outside the ribbon. As expected for photobleaching, most vesicles exhibited a slow decrease in intensity with time. To approximate effects of photobleaching, a linear correction was implemented to correct for this steady decay. After this correction, the standard deviation of vesicle intensities was reduced to 13.7 ± 0.8 for vesicles at the ribbon and 16.4 ± 1.2 away from the ribbon, not significantly different from each other ($P > 0.1$; two-population *t* test). To estimate the contribution of the vesicle alone, the standard deviation in intensity was compared with the standard deviation in intensity when no vesicle is present in the same location in the same cell at a different time. In the absence of a vesicle, the fluorescence had a standard deviation of 11.5 ± 0.6% (mean ± SE) of a vesicle near the ribbon and 11.3 ± 0.5% away from the ribbon. After using these values to correct for the contribution from non-vesicle-associated noise, one gets an estimate of 7.4 ± 1.7% fluctuation in vesicle intensity at the ribbon and 11.9 ± 1.7% away from the ribbon. Given a length constant of excitation light of 50 nm under our conditions, this suggests that these docked vesicles move <3.8 nm at ribbon sites and <6.3 nm when docked away from ribbon sites. Because the fluctuations in intensity due to shot noise increases with brightness, this likely represents an upper limit on the freedom of movement of docked vesicles. Evidently, docking greatly restricts the movement of synaptic vesicles.

During continuous imaging in low calcium, captured vesicles rarely undocked, but such events were much more common away from the ribbon than near the ribbon. In 10 cells, 95 docked vesicles were observed at the membrane for a total of 353 s. Of these vesicles, 39 were found within 700 nm of the center of the ribbon and were observed for a total of 155.9 s. During this time, only one of these vesicles was observed to disappear without undergoing exocytosis. Outside of the ribbon area, undocking events were much more common. Of the 56 vesicles >700 nm away from the ribbon, 14 underwent undocking events in 197.2 s, for a rate of 4.2 $vesicles^{-1}min^{-1}$, 5.5-fold greater than the undocking rate measured at ribbons in the same cells. Spontaneous fusion events were also rare, occurring at 0.77 $vesicle^{-1}$ $min^{-1}$ (two events) at the ribbon, and 1.2 $vesicles^{-1}$ $min^{-1}$ (four events) away from the ribbon. Because phorbol ester phorbol 12-myristate 13-acetate (PMA) has been shown to enhance extrasynaptic release (19), I tested whether PMA also enhanced or stabilized docking of extraribbon vesicles. Application of 100 nM PMA had no significant effect on the rate of undocking at extrasynaptic sites nor on the number of immobilized vesicles. Before treatment with PMA, synaptic terminals had 2.2 ± 0.8 immobilized extraribbon vesicles per 1-s movie ($n = 12$ movies from four cells); after application of 100 nM PMA, cells exhibited 1.9 ± 1.2 spots in the same cells. In the presence of PMA

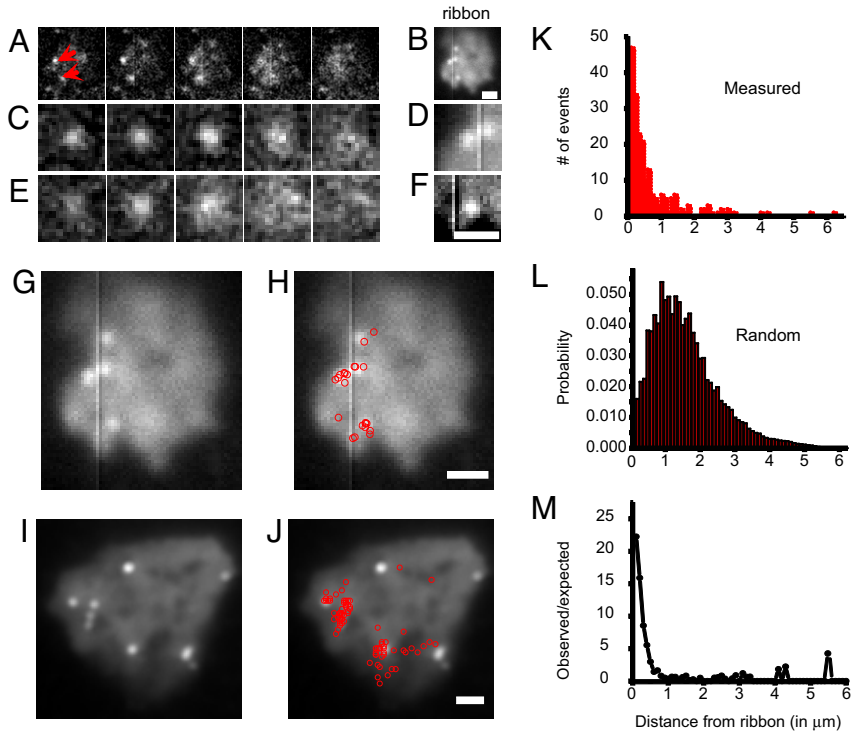


**Fig. 2.** Colocalization between vesicle fusion and ribbon sites. (*A*) A series of consecutive images from the same bipolar cell terminal labeled with FM1–43 and imaged with TIRFM. Images were taken at 33.3 Hz and show the exocytosis of two synaptic vesicles evoked by perfusion of a stimulating solution containing 25 mM KCl and 2.5 mM $CaCl_2$. Red arrows denote the locations of the two vesicles undergoing exocytosis. (*B*) TIRFM image of same cell after introduction of synaptic ribbon-labeling peptide. (Scale bar: 1 $\mu$m.) The scale in *A* is the same as in *B*. (*C* and *E*) Higher magnification of background-subtracted images of vesicles indicated by arrows in *A*. (*D* and *F*) A magnified view of the image in *B*, centered on the same locations as the vesicles in *C* and *E*. Note the proximity of the fusion events in *C* and *E* to ribbon sites in *D* and *F*. (Scale bar: *F*, 1 $\mu$m.) The scale in *C–E* is the same as in *F*. (*G* and *I*) Shown is the ribbon labeling for two different cell footprints imaged by TIRFM. (*H* and *J*) Shown is the same footprint superimposed with the locations of fusion events from the same cell (red circles). (Scale bar: 1 $\mu$m.) (*K*) Histogram of the distances (in micrometers) from fusion events to synaptic ribbons, measured across nine cells. (*L*) Expected distribution of distances from synaptic ribbons to vesicle release sites assuming that release sites are distributed randomly and ribbons are located as measured. The distribution takes into account the shape and size of each cell footprint and is scaled by the number of fusion events for each cell (see *Methods*). (*M*) Ratio of measured distribution of fusion events relative to the ribbon (*K* normalized to the total number of events) to the expectation from a random distribution of fusion events (*L*). Note that after accounting for geometrical constraints, vesicles are most likely to fuse at locations nearest ribbons.

($n$ = four cells), three vesicles undocked in 32 s of imaging for a rate of 5.6 vesicles$^{-1}$ min$^{-1}$. By contrast, spontaneous exocytosis was strikingly increased at extraribbon sites with eight events observed in 42 s of imaging after PMA treatment and one event in 32 s in the same cells before PMA application.

Because the disappearance of vesicles at the ribbon either by spontaneous exocytosis or undocking is such a rare event, time-lapse imaging was used to look over longer periods of time without significant loss of fluorescence through photobleaching. Fig. 3 shows an example from a time-lapse experiment. Single 100-ms exposures were taken at 0.1–2 Hz for several minutes to determine the rate of disappearance of vesicles from the ribbon. In general, vesicles remained fixed at the ribbon while in a low-calcium external solution. In seven cells, 34 vesicles were followed for a total of 53 min. During that time, five vesicles disappeared from the ribbon without a stimulus, for a rate of 0.09 min$^{-1}$. Although for most vesicles it was impossible to determine whether the vesicles underwent spontaneous exocytosis or undocked from the ribbon, two vesicle disappearances were accompanied by a single frame in which a cloud of dye could be clearly distinguished, indicating exocytosis. Thus, vesicles unbound from the ribbon at a rate of less than 0.06 min$^{-1}$. It is also noteworthy that four spontaneous fusion events were detected at locations >500 nm from the ribbon during time-lapse imaging. During time-lapse imaging, bipolar cells were periodically stimulated by using a 25 mM $K^+$/2.5 mM $Ca^{2+}$ solution. In response to this stimulus, 96% ($n$ = 26) of the vesicles present before the stimulus were lost from the ribbon immediately after the stimulus, presumably most because of exocytosis.

**Correlation Between Active Zones and Ribbon Sites.** In previous work, observed clusters of release sites were presumed to represent locations of synaptic ribbons (12, 20). Recent work by the Tachibana laboratory suggests, however, that exocytic events at extraribbon sites also have a nonrandom distribution and that conventional active zones are also present in goldfish retinal bipolar cells (11). Thus, it is of interest to know the degree of error associated with these assumptions. The earlier analysis used a criterion based on the distance from one fusion event to its closest neighboring fusion event to define whether a vesicle is at an active zone or not. Fig. 4 shows a plot of the distance of a vesicle to its nearest neighboring event against the distance to the center of the ribbon for the same vesicle. It is evident from Fig. 4 that most vesicles that occur nearest other events also occur in close proximity to the ribbon. By using a nearest neighbor cutoff of 300 nm to define an active zone (12), one finds that 77 of 88 events (87.5%) that meet that criterion were also within 700 nm of the center of a ribbon. Outlier events based on a nearest neighbor >500 nm away (12) were found to be >700 nm away from the center of the ribbon 81% of the time (25 of 31). Interestingly, the discrepancy between methods is mostly caused by a cluster of events in a single cell, in which an unusually long period separated measurements of exocytosis and ribbon labeling (37 min), suggesting that this cluster may have marked the

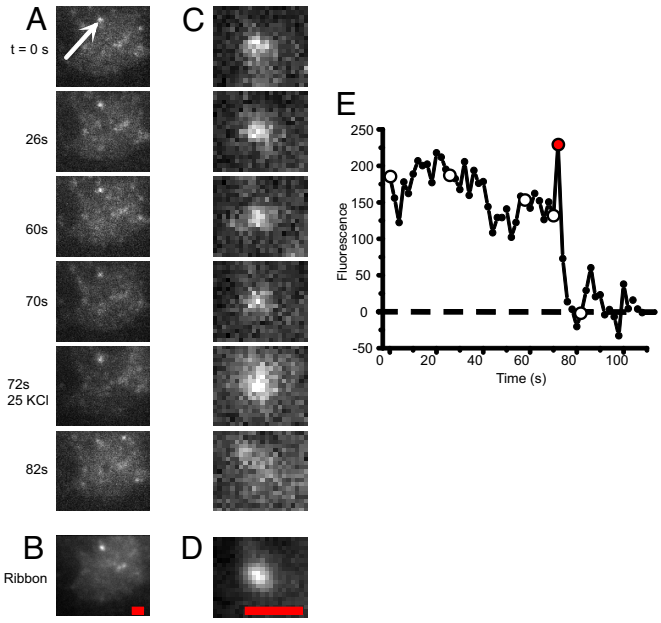


**Fig. 3.** Docked vesicles are retained at the ribbon for long periods. (*A*) TIRFM images from a bipolar cell labeled with FM1–43 and recorded. Representative images of a bipolar cell, which was illuminated and imaged at 0.5 Hz. Times relative to the first image are indicated on the left. Arrow indicates the location of a single vesicle that remains until the cell is stimulated. At 72 s, the cell was locally perfused with a stimulating solution containing 25 mM KCl and 2.5 mM $CaCl_2$ to evoke exocytosis. On perfusion with stimulating solution, vesicle disappears presumably because of exocytosis. (Scale bar: 1 $\mu$m.) (*B*) Image of ribbon labeling from the same cell as in *A*. (*C*) Close-up of the vesicle indicated by the arrow in *A*. (*D*) Same location showing ribbon labeling from the same cell. (*E*) Average fluorescence of vesicle in *C* measured by taking fluorescence in a 675-nm-diameter circular region encompassing the vesicle and subtracting fluorescence from a 675- to 1,500-nm annulus surrounding that circle. Open circles indicate timing of images in *A*. Red circle indicates timing frame in which the cell was stimulated.

location of a ribbon that disappeared in the interim, although we cannot rule out the possibility that this cluster represents a non-ribbon active zone. When data from that one cell are removed, 65 of 68 fusion events within 300 nm of another event were within 700 nm of a ribbon. Evidently, in most cases, proximity to other fusion events is predictive of ribbon location, although some error is introduced by using this criterion.

Recent results from the Tachibana laboratory suggest that extrasynaptic release occurs at non-ribbon active zones in retinal bipolar cells (11). The existence of non-ribbon active zones predicts clustering of release at extraribbon sites as well as at ribbon sites. To look directly at whether extraribbon release is clustered, Fig. 4*C* plots the distance between each extraribbon release event and its nearest neighboring extraribbon event for all cells in this study. Fig. 4*D* plots the expectation for a random distribution taking into account the number of events and footprint shape and size for these cells determined by a Monte Carlo simulation. Notably, Fig. 4*C* lacks the conspicuously left-shifted distribution of Fig. 2*K*. To get an idea of the degree of extrasynaptic clustering of events, one can look at the number of events within 500 nm of another event, approximately the diameter of extraribbon active zones in electron microscopy (11). In total, 33% of the extraribbon events were within 500 nm of other events compared with 27% in the random distribution. Although these data do not rule out the contribution of release at extraribbon active zones, it does strongly suggest that their impact is minimal to the total distribution of events, at least in the absence of phorbol esters.

## Discussion

Taken together the results presented here indicate that the synaptic ribbon locks vesicles in position near release sites for exocytosis. Given the low probability of vesicle unbinding or spontaneous exocytosis, this suggests that once bound to the ribbon, vesicles predominantly leave by stimulated exocytosis. Previous work has suggested that vesicle binding to the ribbon must be near diffusion limited to keep up with measured rates of continuous exocytosis (15). Based on this assumption and the measurements made here, one can get an estimate of the affinity of a vesicle for the ribbon. If association is diffusion-limited, then the association rate of a mobile vesicle with an immobile ribbon is set by the relationship $K_a = (4\pi(r_a + r_b)^*(D_v))$, where $r_a$ and $r_b$ are the radii of the vesicles and ribbon and $D_v$ is the diffusion coefficient of the vesicle. By using typical values for the size of vesicles (40-nm diameter) and ribbon (500-nm diameter) and a diffusion coefficient of 0.015 $\mu m^2/s$ (15), one gets an association rate of $3 \times 10^7$ $M^{-1}$ $s^{-1}$. The results here show that vesicles unbind from the active zones with a rate $<0.001$ $s^{-1}$, for a $K_d$ of $\approx$30 pM. This likely represents an upper bound, because (*i*) undocking and exocytosis are often indistinguishable during time-lapse imaging, (*ii*) by using light microscopy, some extrasynaptic vesicles may be misidentified as ribbon-associated vesicles, and (*iii*) undocking from the ribbon may result from some form of modulation of the binding event rather than reflect the dissociation constant of the vesicle. Of note, the rate of vesicle unbinding and spontaneous exocytosis measured at the synaptic ribbon here is considerably slower than those measured by Murthy and Stevens (1) at hippocampal synapses. In that work, the authors found that vesicles undocked at a rate of $\approx$0.5 $vesicle^{-1}$ $min^{-1}$ and spontaneously underwent exocytosis at a rate of $\approx$0.125 $vesicle^{-1}$ $min^{-1}$. Evidently, the association of the vesicle for the ribbon is a high-affinity interaction. The stability of the vesicle–ribbon interaction may help guarantee stereotyped release rates at the synapse by assuring a constant supply of vesicles at release sites. This interaction must be disrupted during vesicle exocytosis for vesicle protein and/or lipid to be remade into vesicles and for new vesicles to bind to the ribbon; thus, the release of this interaction must be tightly coupled to the exocytic event. It will be of interest to determine what regulates this interaction.

Also of note, spontaneous events appear less tightly restricted to ribbon sites than evoked release. Across the experiments performed here, I detected eight spontaneous events at extraribbon locations and four spontaneous events within 500 nm of a ribbon site under control conditions. Each extraribbon spontaneous event was >700 nm away from the ribbon. By comparison, fusion events >700 nm away from the ribbon made up only 23% of the total evoked events. Despite the small number of spontaneous events, the likelihood of finding 8 of 12 events this far away from the ribbon, assuming a 23% probability, is remote ($P < 0.005$), indicating that spontaneous events are not as tightly correlated to ribbons as evoked events. Recent evidence from hippocampal neurons suggests that spontaneously recycling vesicles and vesicles undergoing evoked release comprise largely independent pools of vesicles (21). The results here suggest that these different pools are also released at different spatial locations. Although the functional significance of our results remains unclear, it may point toward a role of the ribbon for preventing release in the absence of a stimulus as a means of improving signal to noise at the synapse. It should be noted, however, that not all fusing organelles are necessarily synaptic vesicles and one should consider the possibility that some spontaneous events may represent fusion of other organelles (22).

The data here also provide additional evidence for release of vesicles on or near synaptic ribbons. Synaptic ribbons, to which are tethered a dense array of synaptic vesicles, are usually found near voltage-gated calcium channels (16, 20, 23, 24) opposite

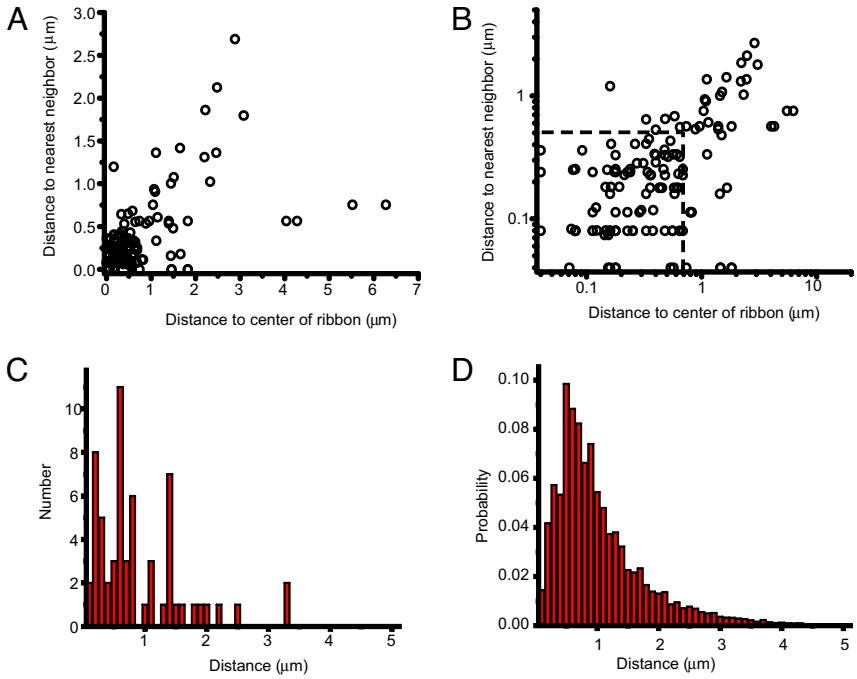


**Fig. 4.** Vesicle clustering predicts ribbon-associated release events. (*A*) Plot of the relationship between interfusion–event distance and distance to synaptic ribbon. Each spot represents a single vesicle. Note the cluster of vesicles near the origin of the plot that represents vesicles that are within 300 nm of another fusion event and 700 nm of the center of a ribbon site, indicating that a large majority of clustered release events are found at sites near the ribbon. (*B*) Same as in *A*, except on both *x* and *y* axes are plotted on logarithmic scales to better visualize individual points. To display all points, all distances <40 nm were assigned a value of 40 nm. Dashed lines enclose the group of vesicles within 700 nm of a ribbon and 500 nm of another fusion event. (*C*) Histogram of distance of fusion events to the nearest neighboring event after events within 700 nm of a ribbon have been removed. Note that histogram of remaining distances fails to exhibit pronounced clustering of release sites. (*D*) Expected distribution of nearest neighbors from a random distribution of vesicles given the number of events and shape of footprint across all cells.

postsynaptic densities and glutamate receptors (2–5). These traits of synaptic ribbons have led to the hypothesis that vesicles attached to these structures represent a releasable pool of synaptic vesicles for exocytosis (25). Along with recently published results from Midorikawa *et al.* (11), I show here direct evidence of synaptic release beneath the ribbon. In addition to ribbon-associated release, Midorikawa *et al.* described extraribbon active zones in electron micrographs that contained postsynaptic densities and a collection of synaptic vesicles, without ribbons (11). In parallel experiments, they showed extraribbon release, which was enhanced by phorbol esters, distributed in a nonrandom manner, that was suggestive of release from these non-ribbon active zones. However, these non-ribbon active zones did not appear to associate with calcium channel clusters (11, 16) and release from these extraribbon sites is delayed relative to ribbon sites possibly because of the need for calcium to diffuse to these locations to activate release (11). These extraribbon active zones are reminiscent of structures described in the bipolar cells of fish, monkey, and salamander (26–28) and may represent a common feature of retinal bipolar cells.

In the experiments presented here, fusion events cluster near ribbons. In addition, extrasynaptic events are still readily apparent, but clusters of events, as defined by locations of two or more release events within 500 nm of one another, occur with only slightly greater frequency than expected from a random distribution. Given that the size of these conventional active zones is smaller than those of ribbons and that these active zones are of similar or lower abundance as ribbons in the cell (11, 28), one would expect a clustering of extraribbon release sites similar to those observed for ribbons sites if release outside the ribbon occurs specifically at these non-ribbon active zones. Instead, my results favor the idea that the extraribbon release primarily occurs at random rather than discrete locations. Instead, the extraribbon clusters of vesicles may mark locations where ribbons previously resided (28).

## Methods

**Cell and Tissue Preparation and Electrical Recording.** Goldfish bipolar cells were isolated as described in ref. 29. In brief, goldfish were decapitated and eyes were removed and hemisected. To remove vitreous, eyecups were placed for 20 min in a solution of hyaluronidase (1,100 units/ml) containing 120 mM NaCl, 0.5 mM $CaCl_2$, 2.5 mM KCl, 1 mM $MgCl_2$, 10 mM glucose, and 10 mM Hepes. Next, each retina was removed from the eyecups and cut into six to eight pieces and digested in a papain (30 units/ml; Fluka) solution for 35 min containing 2.7 mM cysteine, 120 mM NaCl, 0.5 mM $CaCl_2$, 2.5 mM KCl, 1 mM $MgCl_2$, 10 mM glucose, and 10 mM Hepes. Pieces of tissue were mechanically triturated by using a fire-polished Pasteur pipette and plated on to high refractive index coverslips ($n_{488}$ = 1.80; Plan Optik). Bipolar neurons were recognized by their unique morphology and used within 8 h of removing the retina. For imaging experiments, cells were placed in a low-calcium imaging solution containing 120 mM NaCl, 0.5 mM $CaCl_2$, 2.5 mM KCl, 1.0 mM $MgCl_2$, 0.75 mM EGTA, 10 mM glucose, 10 mM Hepes, and either 1 mM ascorbic acid or 1 mM glutathione to reduce phototoxicity. Solution was adjusted to pH 7.4 by using NaOH.

Bipolar cells were voltage-clamped by using an EPC-10 amplifier (Heka Electronik), running Pulse (Instrutech) stimulus and acquisition software. The patch pipette was placed on the cell body and the pipette solution contained 120 mM Cs-gluconate, 4 mM $Na_2ATP$, 0.5 mM GTP, 4 mM $MgCl_2$, 10 mM TEA-Cl, 0.5 mM EGTA, 10 mM Hepes (pH 7.2 with CsOH), and 50 $\mu$M synthetic peptide (HyLite488-EQTVPIDLSERDR; Anaspec) which specifically binds to synaptic ribbons (16) and is synthesized with an N-terminal fluorophore.

**Fluorescence Imaging.** To image vesicles, bipolar cells were loaded with the styryl dye FM1–43 (13, 30) modified from a protocol described to specifically load synaptic vesicles with the dye (12, 22). Specifically, bipolar cells were labeled with a 10-s local application of a modified Ringer's solution containing 95 mM NaCl, 2.5 mM $CaCl_2$, 25 mM KCl, 1.0 mM $MgCl_2$, 10 mM glucose, 10 mM

Hepes (pH 7.4 with NaOH) with a pulled, thin-walled glass pipette (World Precision Instruments). After application of the FM1–43-containing solution, the cells were washed in a dye-free low-calcium imaging solution (contents as listed earlier) for 25–45 min before imaging. Cells were kept in this low-calcium solution for the duration of these experiments, except when loading with FM1–43, stimulated to evoke exocytosis (see below) or for whole-cell voltage clamp.

Cells were viewed through an inverted microscope (Olympus IX70) modified for through-the-lens evanescent field illumination (31, 32) as described in ref. 29. A 20-mW (run at 20–40% power) 488-nm wavelength beam from a solid-state laser (Sapphire 488; Coherent) was applied by opening and closing a shutter during periods of observation. The beam was passed through a linear polarizer and focused off-axis onto the back focal plane of a 1.65 NA objective (Apo ×100 O HR, Olympus). After leaving the objective, light traveled through a high refractive index immersion fluid (Series M, $n_{488} = 1.81$; Cargille Laboratories) then entered a coverslip of high refractive index glass ($n_{488} = 1.80$) and underwent total internal reflection as it struck the interface between the glass and the solution or cell. Fluorescence images were acquired by using intensified CCD cameras (Cascade 650 and Cascade 512B, Roper Scientific). Data were collected and analyzed by using Metamorph acquisition and analysis software (Molecular Devices).

To stimulate exocytosis, bipolar cells were locally perfused by manually applying pressure to a thin-walled glass pipette located 20–30 $\mu$m from the synaptic terminal and containing a solution of 95 mM NaCl, 2.5 mM $CaCl_2$, 25 mM KCl, 1.0 mM $MgCl_2$, 10 mM glucose, 10 mM Hepes (pH 7.4 with NaOH).

**Analysis.** Vesicles were identified by visual observation and fit to the 2D Gaussian function, $\exp(-r^2/w^2)$, where $r$ is the distance from the center of the object and $w$ is the width parameter. Across 100 visually identified vesicles, $w$ averaged 211 ± 11 nm. This is strikingly similar to the width parameter measured for 20-nm-diameter beads labeled with FM1–43 (215 ± 23 nm; $n = 11$), consistent with spots being diffraction limited in size as expected for a synaptic vesicle. Vesicle intensities were measured by averaging the fluorescence in a 675-nm-diameter circular region centered on the vesicle and subtracting the average fluorescence in an annular region with an inner diameter of 675 nm and an outer diameter of 1,500 nm.

To determine the expected distance to ribbons given a random distribution of vesicles, footprints of bipolar cell terminals loaded with a fluorescent peptide were first converted into binary images where regions outside the footprint were assigned a value of 0 and footprint-associated pixels were assigned a value of 255. A text file containing the pixel values for this binarized image was read into a qbasic program written to measure the distance from each nonzero pixel location to the coordinates of observed ribbons. This program returned a file that contained the pixel-to-ribbon distances, which were used to generate a histogram of distances to each cell. Each histogram was divided by the total number of nonzero pixels to normalize to the number of pixels in each footprint. To arrive at the graph in Fig. 3*E*, normalized histograms for each cell were weighted by the number of fusion events that were observed in that cell.

Some movement of the stage and/or cell sometimes occurred in the interval between the imaging of vesicles and the introduction of the ribbon-labeling peptide or between streams of vesicle imaging. To correct for any movement, binary images generated of averages from movies were used to visually align terminal footprints by using the ''color align'' utility on Metamorph. In one case, changes in footprint shape with time made alignment unreliable and this cell was not used in the analysis for this article.

**ACKNOWLEDGMENTS.** This work was supported by National Eye Institute Grant EY014990 and a scholar award from the McKnight foundation.

1. Murthy VN, Stevens CF (1999) Reversal of synaptic vesicle docking at central synapses. *Nat Neurosci* 2:503–507.
2. Morigiwa K, Vardi N (1999) Differential expression of ionotropic glutamate receptor subunits in the outer retina. *J Comp Neurol* 405:173–184.
3. Qin P, Pourcho RG (1999) Localization of AMPA-selective glutamate receptor subunits in the cat retina: A light- and electron-microscopic study. *Vis Neurosci* 16:169–177.
4. Matsubara A, Laake JH, Davanger S, Usami S, Ottersen OP (1996) Organization of AMPA receptor subunits at a glutamate synapse: A quantitative immunogold analysis of hair cell synapses in the rat organ of Corti. *J Neurosci* 16:4457–4467.
5. Ghosh KK, Haverkamp S, Wassle H (2001) Glutamate receptors in the rod pathway of the mammalian retina. *J Neurosci* 21:8636–8647.
6. Heidelberger R, Thoreson WB, Witkovsky P (2005) Synaptic transmission at retinal ribbon synapses. *Prog Retin Eye Res* 24:682–720.
7. Sterling P, Matthews G (2005) Structure and function of ribbon synapses. *Trends Neurosci* 28:20–29.
8. Usukura J, Yamada E (1987) Ultrastructure of the synaptic ribbons in photoreceptor cells of Rana catesbeiana revealed by freeze-etching and freeze-substitution. *Cell Tissue Res* 247:483–488.
9. Gray EG, Pease HL (1971) On understanding the organisation of the retinal receptor synapses. *Brain Res* 35:1–15.
10. Bunt AH (1971) Enzymatic digestion of synaptic ribbons in amphibian retinal photoreceptors. *Brain Res* 25:571–577.
11. Midorikawa M, Tsukamoto Y, Berglund K, Ishii M, Tachibana M (2007) Different roles of ribbon-associated and ribbon-free active zones in retinal bipolar cells. *Nat Neurosci* 10:1268–1276.
12. Zenisek D, Steyer JA, Almers W (2000) Transport, capture and exocytosis of single synaptic vesicles at active zones. *Nature* 406:849–854.
13. Betz WJ, Bewick GS (1992) Optical analysis of synaptic vesicle recycling at the frog neuromuscular junction. *Science* 255:200–203.
14. Rouze NC, Schwartz EA (1998) Continuous and transient vesicle cycling at a ribbon synapse. *J Neurosci* 18:8614–8624.
15. Holt M, Cooke A, Neef A, Lagnado L (2004) High mobility of vesicles supports continuous exocytosis at a ribbon synapse. *Curr Biol* 14:173–183.
16. Zenisek D, Horst NK, Merrifield C, Sterling P, Matthews G (2004) Visualizing synaptic ribbons in the living cell. *J Neurosci* 24:9752–9759.
17. Zenisek D, Matthews G (1998) Calcium action potentials in retinal bipolar neurons. *Vis Neurosci* 15:69–75.
18. Protti DA, Flores-Herr N, von Gersdorff H (2000) Light evokes $Ca^{2+}$ spikes in the axon terminal of a retinal bipolar cell. *Neuron* 25:215–227.
19. Midorikawa M, Tsukamoto Y, Berglund K, Ishii M, Tachibana M (2007) Different roles of ribbon-associated and ribbon-free active zones in retinal bipolar cells. *Nat Neurosci* 10:1268–1276.
20. Zenisek D, Davila V, Wan L, Almers W (2003) Imaging calcium entry sites and ribbon structures in two presynaptic cells. *J Neurosci* 23:2538–2548.
21. Sara Y, Virmani T, Deak F, Liu X, Kavalali ET (2005) An isolated pool of vesicles recycles at rest and drives spontaneous neurotransmission. *Neuron* 45:563–573.
22. Coggins MR, Grabner CP, Almers W, Zenisek D (2007) Stimulated exocytosis of endosomes in goldfish retinal bipolar neurons *J Physiol* 584:853–865.
23. Issa NP, Hudspeth AJ (1996) The entry and clearance of $Ca^{2+}$ at individual presynaptic active zones of hair cells from the bullfrog's sacculus. *Proc Natl Acad Sci USA* 93:9527–9532.
24. Roberts WM, Jacobs RA, Hudspeth AJ (1990) Colocalization of ion channels involved in frequency selectivity and synaptic transmission at presynaptic active zones of hair cells. *J Neurosci* 10:3664–3684.
25. von Gersdorff H, Vardi E, Matthews G, Sterling P (1996) Evidence that vesicles on the synaptic ribbon of retinal bipolar neurons can be rapidly released. *Neuron* 16:1221–1227.
26. Grunert U, Haverkamp S, Fletcher EL, Wassle H (2002) Synaptic distribution of ionotropic glutamate receptors in the inner plexiform layer of the primate retina. *J Comp Neurol* 447:138–151.
27. Wong-Riley MT (1974) Synaptic organization of the inner plexiform layer in the retina of the tiger salamander. *J Neurocytol* 3:1–33.
28. Hull C, Studholme K, Yazulla S, von Gersdorff H (2006) Diurnal changes in exocytosis and the number of synaptic ribbons at active zones of an ON-type bipolar cell terminal. *J Neurophysiol* 96:2025–2033.
29. Zenisek D, Steyer JA, Feldman ME, Almers W (2002) A membrane marker leaves synaptic vesicles in milliseconds after exocytosis in retinal bipolar cells. *Neuron* 35:1085–1097.
30. Betz WJ, Bewick GS, Ridge RM (1992) Intracellular movements of fluorescently labeled synaptic vesicles in frog motor nerve terminals during nerve stimulation. *Neuron* 9:805–813
31. Axelrod D (2001) Total internal reflection fluorescence microscopy in cell biology. *Traffic* 2:764–774.
32. Steyer JA, Almers W (2001) A real-time view of life within 100 nm of the plasma membrane. *Nat Rev Mol Cell Biol* 2:268–275.